Geomechanics and Engineering, *Vol. 29, No. 4 (2022) 463-470*
https://doi.org/10.12989/gae.2022.29.4.463

Technique of grouting in silty-fine sand with abundant water: Practice in Beijing

Jun Liu*[1], Liang Zhang[1], Hongsong Xue[2], Tian You[1] and Yuqian Wu[1]

[1]*School of Civil and Transportation Engineering, Beijing University of Civil Engineering and Architecture, Beijing 100044, China*
[2]*BCEG Civil Engineering co.,LTD, Beijing 100044, China*

(Received April 4, 2019, Revised February 6, 2022, Accepted March 11, 2022)

Abstract. In NATM tunnels, water inrush and tunnel collapse are often encountered in silty-fine sand with abundant water during excavation. Because of the special engineering properties of this stratum, grouting effect is difficult to achieve as expected, and it is a major problem in the field of civil engineering. Taking Beijing Metro Line 10 as a case, we applied PFC3D to simulate the process of grouting in this stratum. By analyzing the law of grout diffusing and porosity change under different grouting pressures, the study found that grouting was a process of splitting, and grouting pressure played an important role. The numerical results were verified by theoretical calculation analysis, and the grouting parameters were determined under the various grouting pressures for practice. After the excavation of this tunnel, the concretions in silty-fine sand are similar to the results of PFC3D simulation, which indicates that the grouting mechanism is confirmed by field observation further.

Keywords: grounting pressure; NATM tunnel; silty-fine sand with abundant wate; splitting grounting

1. Introduction

In tunnel practice, the silty-fine sand with abundant water is often encountered. After excavation, the water and sand can gush into the tunnel and may cause tunnel collapse, which affects the safety of surrounding environment, so it must be treated before excavation. Grouting is a process that the grout is injected into the soil by grouting equipment, and forms concretions after its solidification. Because the grouted soil has characteristics of high strength and waterproof, this method can improve the soil effectively. Therefore, the grouting has been widely employed in civil engineering (Stille *et al.* 2012, Loveridge and Powrie 2014, Do *et al.* 2014).

Recently, many scholars have carried out deep research on permeating grouting, compactin g grouting and splitting grouting, and they put forward a series of grouting theory and practice. Bjrn and Gustafson (2010) introduced the application of grouting technology in Botnabana railway tunnel project in northern Sweden, which suggested a different approach to hydrogeological prognosis and the grouting process, such as distribution of grouting classes, increase of mixer capacities and regular use of two grouting rounds. Kim *et al.* (2013) investigated the interaction of pressure grouting and the basic properties of the grout, through a series of laboratory tests performed on specially designed. Silva *et al.* (2016) studied the mechanical behavior of the soil after grouting, and concluded that the injection had achieved satisfactory recovery of shear strength. Dong-MeiZhang *et al.* (2018) analyzed the feasibility of grouting in controlling the subsidence of soft tunnel stratum by introducing an engineering example of a double O-shaped tunnel in Shanghai. Fatih Cel (2019) summarized some parameters affecting the results of cement-based permeation grout, such as rheological properties, permeability coefficient of cement slurry and injectability of cement slurry.

However, there are essential differences between silty-fine sand with abundant water and Loess, clay, pebble soil and other strata (Jun *et al.* 2015). As a type of sands, the silty-fine sand has small particle size and uniform particle composition, and the grouting is often considered as permeation grouting. But, the engineering properties of silty-fine sand are between sandy soil and cohesive soil, and the permeability coefficient is generally 1.0×10-3 cm/s, so the slurry is very difficult to infiltrate, especially in abundant water condition, which leads to more engineering accidents in tunnel excavation (Hang *et al.* 2017, Le *et al.* 2019). These accidents may be due to the complexity and concealment of underground grouting process, involving many imperfect disciplines such as rock, soil, fluid, materials, etc., especially for the grouting study of silty-fine sand with abundant water, which lacks theoretical support of practical engineering (Bezuijen *et al.* 2011). This paper studied the process of grouting in silty-fine sand with abundant water by PFC3D and revealed the mechanism of grouting, and believed that grouting pressure played an important role in the process of grouting. The numerical results were verified by theoretical calculation analysis, and the grouting parameters were determined under the various grouting pressures. After the excavation of this tunnel, the concretions in silty-fine sand are similar to the results of PFC3D simulation, which indicates that the grouting mechanism is confirmed by field observation further and has important significance for guiding future grouting practice in similar stratum.

*Corresponding author, Professor
E-mail: Liujun@bucea.edu.cn

ISSN: 2005-307X (Print), 2092-6219 (Online)

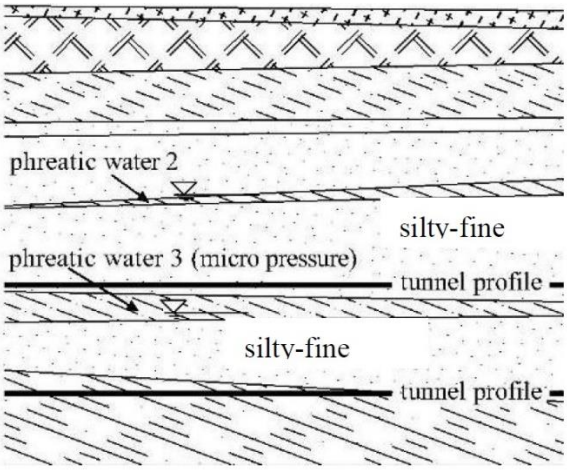

Fig. 1 Schematic diagram of engineering geological section

Fig. 2 Photo of the gushing water and sand from shaft side wall

2. Engineering survey

The tunnel of Beijing Metro Line 10 is constructed by the NATM method, and the tunnel top cover soil is about 17.5 m~ 18.5 m. The stratum of the tunnel is mainly thick silty-fine sand with abundant water, there are three kinds of underground water, the top is not associated with the excavation of NATM tunnel, the two others are the area of this NATM tunnel (Fig. 1), and the water pressure is about 0.22 MPa obtained by field test. Besides, there are many buildings and underground pipelines around the tunnel.

In early practice of grouting, we grouted this stratum based on the mechanism of permeation grouting. After grouting was completed, the gushing of water and sand (Fig. 2) occurred in the excavation shaft, so the further excavation had to be terminated, and the new method had to be taken into considered.

3. PFC^{3D} simulation

3.1 PFC^{3D} simulation principle

Three-dimensional particle flow (PFC3D) discrete element program is used for simulations. The model of 4 adjacent particles to form a "area", adjacent to the region through the "conduit" connection, and its pore size and the distance between the particles is related to the relative movement of the liquid in the pipe flow (Kodam *et al.* 2009).

When the pressure in the pipe is high, there is an outward force on the surrounding area. The ends of the pipe are fluid regions, and there is a pressure difference between the adjacent regions. When the fluid solid coupling is calculated, the fluid in the adjacent area occurs "flow", and it also acting on the surrounding particles, thus simulating the function of the grout entering the soil mass. Therefore, the program simulates fluid motion through fluid region and pipe, and then carries out fluid-solid coupling calculation.

In the PFC^{3D} program, the flow velocity q is given by the formula (1) when the grout is passed through the pipe

$$q = ka^3 \frac{P_2 - P_1}{L} \tag{1}$$

where k is the conduction factor, L is the length of pipe that is distance between two adjacent regions, a is the diameter of the pipe, (P_2-P_1) is the pressure difference between two adjacent regions.

The following is an empirical formula used for calculating the diameter of the pipe, which is between a0 and 0. The formula can be expressed as

$$a = \frac{a_0 F_0}{F + F_0} \tag{2}$$

In the above, a_0 indicates the aperture of pipe when the normal force is zero, 0 indicates the normal force tends to infinity, F_0 is the normal force (when pressure is positive), F is the normal force when the aperture of pipe is reduced to a/2.

The increment in grout pressure ΔP can be obtained by the following expression (assuming the inflow is positive):

$$\Delta P = \frac{K_f}{V_d}(\sum q\Delta t - \Delta V_d) \tag{3}$$

Where K_f is grout bulk modulus, V_d is the apparent volume of the region, ΔV_d is the change in the volume of the area affected by force, Δt is a calculate time step.

The inflow or outflow of each area due to the pressure disturbance ΔP_p can be calculated by formula (4)

$$q = \frac{Nka^3 \Delta p_p}{\bar{l}} \tag{4}$$

where $\bar{l}$ is the average distance between the area and adjacent areas, N is the number of pipes connected to the area.

According to formula (5), the pressure response caused by this flow can be calculated by

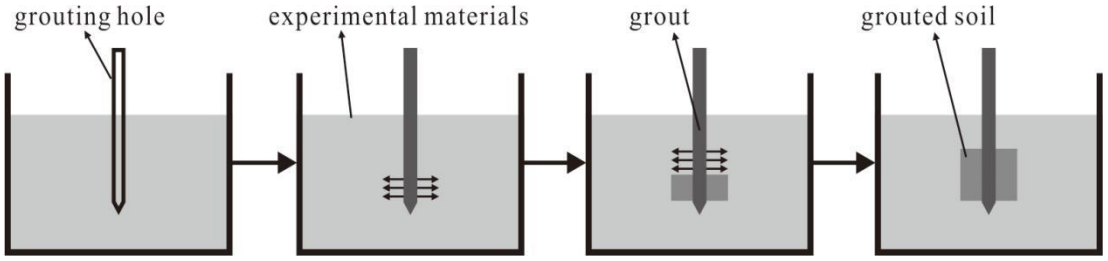

Fig. 3 Sleeve valve pipe grouting process

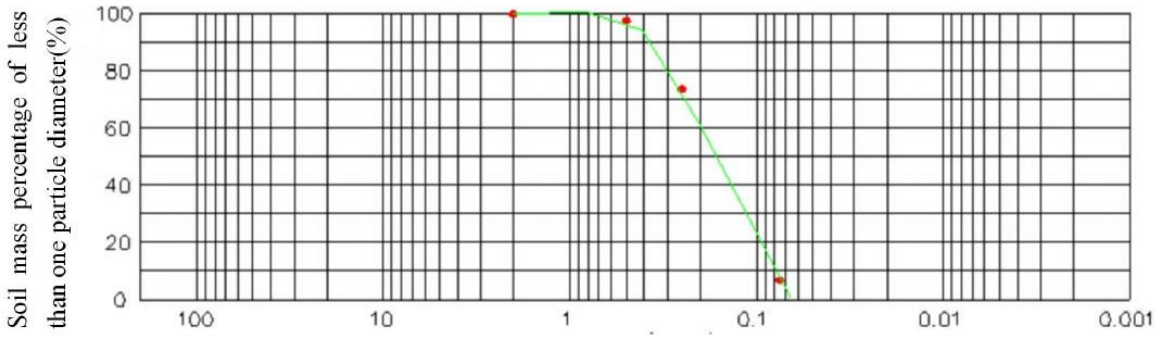

Fig. 4 Grains gradation curve

Table 1 Particle analysis and particle composition indicators

Grain size distribution (mm)	>2 mm	2~0.5	0.25~0.075	0.075~0	$d_{60}=0.196$	$C_u=\frac{d_{60}}{d_{10}}=2.450$
					$d_{30}=0.114$	
Proportion	2.3%	23.9%	66.9%	6.7%	$d_{10}=0.080$	$C_c=\frac{d_{30}^2}{d_{10}\times d_{60}}=0.829$
					$d_5=0.087$	

$$\Delta p_r = \frac{K_f q \Delta t}{V_d} \tag{5}$$

In order to insure the convergence of calculation, the pressure response should be less than the initial pressure disturbance (Amnieh *et al*. 2017). From formula (4) and (5), we can obtain

$$\Delta t \le \frac{\bar{I}V_d}{NK_f k a^3} \tag{6}$$

In the above calculation, there are three types of fluid and solid particles. First, the change of the pore is defined by the contact switch, or the change of the contact force. Secondly, the mechanical changes of the regional volume cause the change of the fluid pressure in the region. Thirdly, the regional pressure has an action on the surrounding particles. Therefore, the contact force acting on a typical particle can be expressed as follows

$$F_i = pn_i s \tag{7}$$

where p is the pressure within an area, n_i is unit normal vector, s is the projected area between one particle and the adjacent three particles in an area.

3.2 Model and calculation parameters

The model is designed based on the principle of sleeve valve pipe grouting, the grouting process can be seen in Fig. 3. The experimental materials for model are silty-fine sand from Beijing Metro Line 10. Particle-size analysis indicated that the sand particle size was in a range of 2.0 mm~0.075 mm with the clay content about 6.7% as shown in Table 1. and Fig. 4. In addition, the permeability coefficient was about 2.0×10^{-3} cm/s tested in the field.

The number of particles has a certain influence on the simulation results and calculation efficiency. When the number of particles reaches hundreds of thousands or even millions, the calculation speed will decrease significantly. Therefore, it is necessary to consider controlling the number of particles produced (Sadek *et al*. 2011). In the PFC^{3D} numerical simulation analysis, the model size (Fig. 5) is 5 m×5 m×5 m. The grey and green colors indicate sand soil

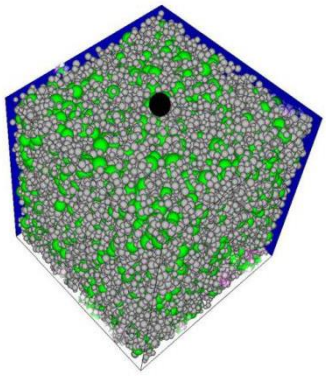

Fig. 5 The model of PFC3D numerical simulation

Table 2 The parameters used for PFC3D numerical simulation

The fine-sand with abundant water particles	
Particle size	0.075 mm~2.0 mm
Friction coefficient	0.2
Porosity	0.30
Density	26 kN/m^3
Parallel connection strength	5×10^5 N/m^2
Normal /tangential stiffness	1.8×10^7 N/m
Poisson's ratio	0.28
Fluid	
Density	1×10^3 kN/m^3
Viscous coefficient	1.01×10^{-3} Pa.s
Calculation parameters	
Gravity acceleration	9.81 m/s^2
DEM calculation time step	5.206×10^{-6}s
CFD calculate time step	3.5×10^{-5}s

generated by 9934 particles which are randomly distributed. The black represents the location of grouting hole. The blue is an impermeable boundary with enough rigidity to prevent the sand particles flying out off the model.

The parameters used for PFC^{3D} simulation are obtained from the field and the laboratory test, which are shown in Table 2.

3.3 Analysis of calculation results

The calculation model does not consider the contact strength between sand grains, which is similar to the properties of sand. There is no cohesion between the grains. The parallel connection strength between the grains is set up, that is to say, the cohesion effect is considered. The form of grout seepage diffusion is analyzed by changing grouting pressures. Four grouting pressures (i.e., 0.5 MPa, 0.75 MPa, 1.0 MPa and 1.25 MPa) are selected in the simulation, which aims at analyzing the grout moving and porosity change in silty-fine sand after grouting.

3.3.1 Grout moving track under different pressures

At the grouting pressure of 0.5 MPa (Fig. 6(a)), the injected grout is gathered around the grouting hole and forms some grout bubbles, which produces extrusion force on the surrounding silty-fine sand, and the radius of compressive zone is about 0.3 m. The link between the particles is not broken at this pressure, but the contact stress concentration increases.

With the increase of grouting pressure up to 0.75 MPa (Fic. 6(b)), the radius of compressive zone expanded to 0.4m, the contact stress chains tend to be banding.

Fig. 6 shows the moving track of the grout (red color) under different grouting pressures.

When the pressure reaches 1.0 MPa (Fig. 6(c)), the fissures occur along the plane which is perpendicular to the minimum principal stress. The fissures are randomly spread around the hole with a radius about 0.5 m, that is, the pressure exceed the initial stress and tensile strength of silty-fine sand, and this indicates the grouting pressure runs up to the fracture pressure. After solidification of the grout, the grouting concretions are formed in the shape of the vein and star point or block.

When the grouting pressure reaches 1.25 MPa (Fig. 6(d)), the maximum principal stress is horizontal at this moment. The fissures begin to develop in the vertical direction around the hole within a radius of 0.7 m. Similarly, the grouting concretions are formed in the shape of the vein and star point or block after grout solidification.

3.3.2 Porosity change analysis

The porosity of soil is the ratio of the total volume of soil, and the porosity is one of the most important indexes in geotechnical engineering (Cho *et al.* 2004). The sum of the porosity and compactness is 1, so the porosity can reflect the degree of soil compaction.

In order to further analyze change of the silty-fine sand density in grouting, using the measure circular command of software PFC^{3D}. By analyzing the changes of the porosity in the range to analyze density changes. Taking the grouting pressure 1.0MPa as an example, the measure circle diameter of 1.0 m, 2.0 m, 3.0 m, 4.0 m and 5.0 m were selected as the center of the grouting hole, and the change of the com pactness of soil around the grouting hole was analyzed. Sand soil porosity varies with the time step was shown in Fig. 7 where the abscissa represented time step and ordinate represented porosity changes in the measurement circle. In this calculation, the 850 step is calculated from 1.215×10^4 to 1.300×10^4, and the porosity of the second half of the curve tends to be stable, which indicates that the selected calculation is reasonable. Diagram has 5 curves, serial numbers from 1 to 5 with different colors, respectively, corresponding to the diameter of the circle from 5.0 m to 1.0 m.

When the diameter of the measurement circle is about 1.0 m, the porosity tends to be increased, changing from 33.3% to 34.9%, increased by about 5%. The closer to the center of the grouting hole, the more obvious the porosity is increased. The phenomenon indicates that the silty-fine sand in this place has been disturbed, the filling and splitting occur, and more pores and fissures have been produced. In other word, the amount of injected grout here is large, the bubbles and the veins can be formed after grout solidification.

When the diameter of the measurement circle is about 2.0 m, the increase of porosity is very small, changing from

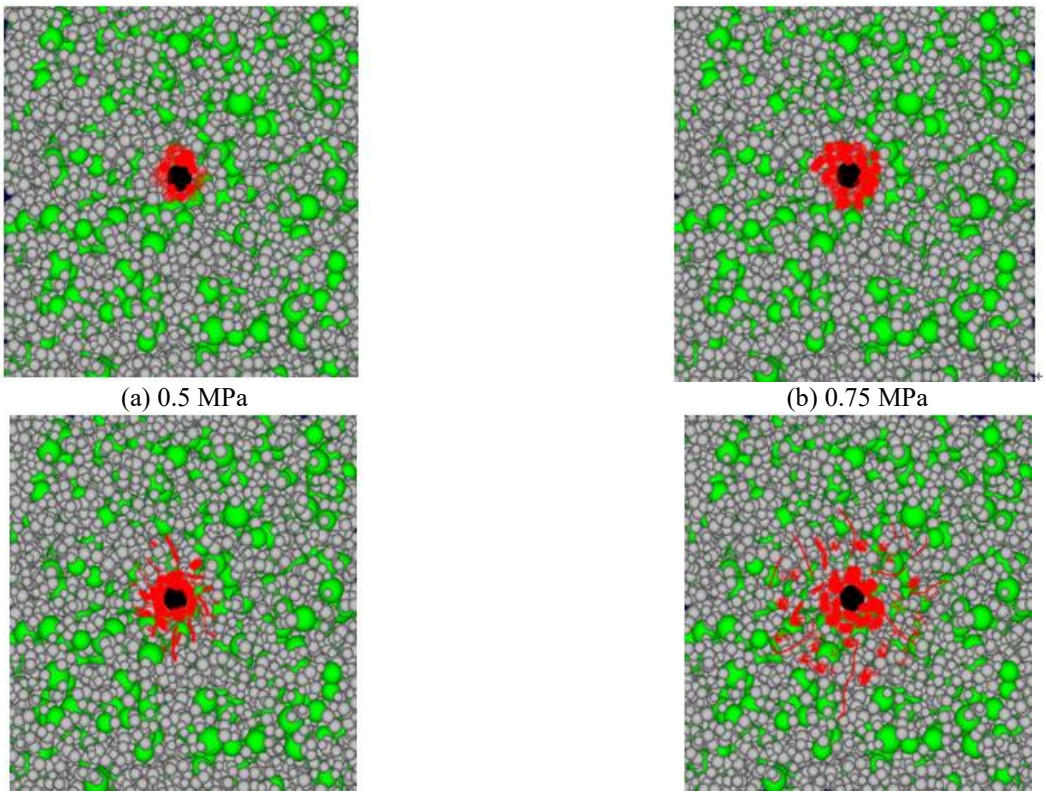

(a) 0.5 MPa (b) 0.75 MPa

(c) 1.0 MPa (d) 1.25MPa

Fig. 6 Grout moving track

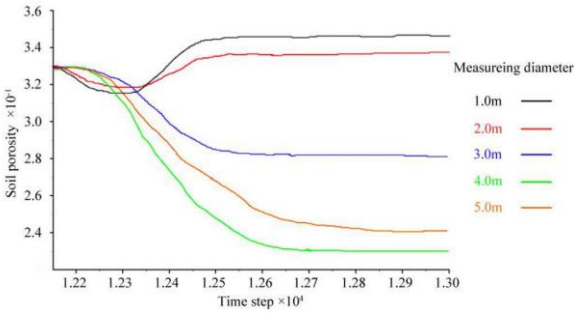

Fig. 7 The diagram of the changes of density at 1.0 MPa

33.3% to 33.5%. The area may be the transition zone from the splitting to compacting, and the branch or star point may occur.

When the diameter of the measurement circle is from 3.0 m to 5.0 m, some significant changes occur in the trend of the curve, that is, the significant reduction of the porosity appears. Within the diameter of 3.0 m, the porosity is decreased from 33.3% to 27.9%, decreased by about 16.2%; within the diameter of 4.0m, the porosity is decreased from 33.3% to 23.2%, decreased by about 30.3%; within the diameter of 5.0 m, the porosity is decreased from 33.3% to 24.2%, decreased by about 27.9%.

From the changes of porosity, it shows clearly that the main zone of grouting in silty-fine sand is within the radius of 0.5 m around the hole, the soil has been disturbed strongly here, and some grouting concretions may be formed in the shape of the block and vein. Within the radius of 1.0 m, some grouting concretions like the branch vein or star point may be formed also. Outside of the radius of 1.0 m, the silty-fine sand is compacted, in other word, the silty-fine sand has been improved in a degree.

4. Practice in Beijing

4.1 Grouting parameters

The PFC^{3D} simulation study found that fracture grouting should be adopted to achieve the grouting effect, and a new grouting scheme using sleeve valve tube was formulated.

1) Grouting pressure

According to PFC^{3D} simulation, the grouting pressure of fracture grouting is very important. When the grouting pressure is less than initiation fracture pressure, the grouting fluid will converge near the grouting hole to form a grouting bubble. When the grouting pressure exceeds fracture initiation pressure, the grouting bubble will break and the grouting fluid will flow in a fracture mode.

The fracture initiation pressure in sandy soil can be calculated according to Coulomb-Mohr failure criterion of effective stress, as shown in Eq. (8)

$$\frac{\sigma_1+\sigma_3}{2}\cdot\sin\varphi=\frac{\sigma_1-\sigma_3}{2}-C\cdot\cos\varphi \tag{8}$$

Where σ_1 is the major principal stress and σ_3 is the minor principal stress. The buried depth of the project is about 18

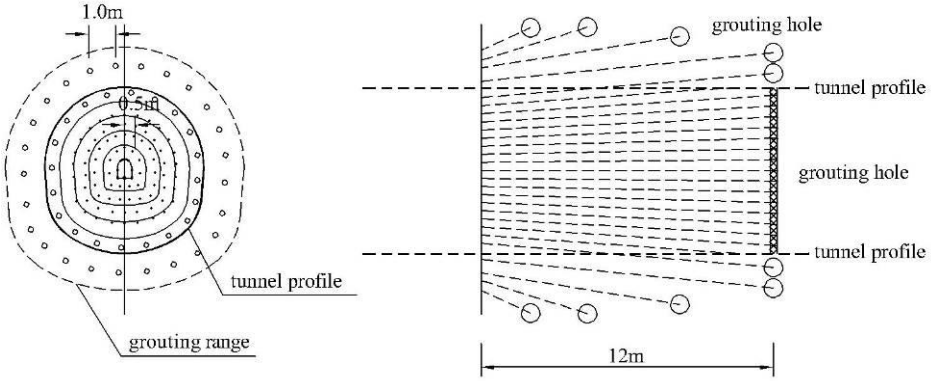

Fig. 8 Layout of grouting holes

m, so the maximum principal stress is equivalent to 0.324 MPa. Where C is the cohesion, approximate to 0, and the frictional angle φ is taken as 25 degrees.

According to formula (8), the minimum principal stress is 0.132 MPa and the principal stress ratio (σ_1/σ) is 2.46.

The initiation fracture pressure P_u can be obtained by:

$$P_u = (\gamma h - \gamma_w h_w)\cdot(1+K) - \frac{(\gamma h - \gamma_w h_w)\cdot(1-K)}{\sin\varphi} + 2C\cdot\cos\varphi \qquad (9)$$

where γ, γ_w are the unit weight of sand and water respectively, which are about 18 kN/m^3 and 10 kN/m^3, and the depth of grouting hole h is 18 m, the depth of groundwater h_w is about 18 m. K is principal stress ratio which is 2.46.

According to formula (9), P_u can be calculated as 0.76 MPa. The pore water pressure of 0.22 MPa is not taken into considered in this result. In actual, P_u is the sum total of them as mentioned above, which is about 0.98 MPa. The result agrees with that of PFC^{3D} simulation, therefore the initiation fracture pressure is proposed to be 1 MPa.

2) The design of grouting holes

In order to get a better effect of water stop and reinforcement during grouting, the whole section of this tunnel was designed for the grouting holes. The grouting reinforcement area was 3 m~5 m beyond the excavation contour line of tunnel, and the grouting holes were presented as a pattern in umbrella-type along the tunnel.

The spacing of grouting holes was about 0.5 m (Fig. 8), and the length of each grouting cycle was 12 m along the tunnel, the blind area of grouting was able to be eliminated by using both long and short grouting pipes.

3)The grouting speed and the final grouting pressure

If the injected grout was less than 2L/min or one hole nearby gushes grout, the grouting should be stopped. The pressure of ending the grouting is so called the final grouting pressure, which is often larger than 1.0MPa.

4.2 Grouting process

Taking grouting hole 1 as an example, the measured curve of grouting pressure-amount-time is shown in Fig. 9. In the process of grouting, the grouting amount gradually reduces from 8L/min to 1L/min, and the grouting pressure gradually increases from 1.0 MPa to 1.5 MPa, so the final grouting pressure is about 1.5 MPa.

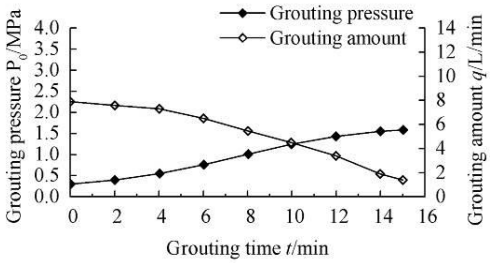

Fig. 9 Grouting pressure-grouting velocity-grouting time curve of hole 1

After the consolidation of grout, some tests were performed. One was packer test for permeability by water injection in the field, and the permeability coefficient of the silty-fine sand was between 3×10^{-6}cm/s-4.3×10^{-6}cm/s. Another was core drilling for laboratory test, the samples were cylinder with the diameter of 10cm, and the total of the samples were 6 which were obtained from the whole section of the tunnel. The samples were intact and had many concretions of grout, the average of unconfined compressive strength was about 0.54 MPa. The results were satisfied with the design value of grouting, that is, the permeability coefficient was less than 1×10^{-5}cm/s and the unconfined compressive strength was larger than 0.5 MPa.

In order to verify the results as mentioned above, every detail of soil reinforcement and leakage water after the excavation of this tunnel were monitored. The observations indicated that there were little leakage water and the silty-fine sand was compact at the place of the tunnel face and vault. The concretions of grout are shown in Fig. 10. Fig. 10(a) is the grout bubble, Fig. 10(b) is the grout vein, Fig. 10(c) is the grout vein and star point. The concretions of grout observed from field are almost identical with the results of PFC^{3D} simulation.

5. Discussions

From the simulation of PFC^{3D} and practice in Beijing, the grouting in the silty-fine sand with with abundant water

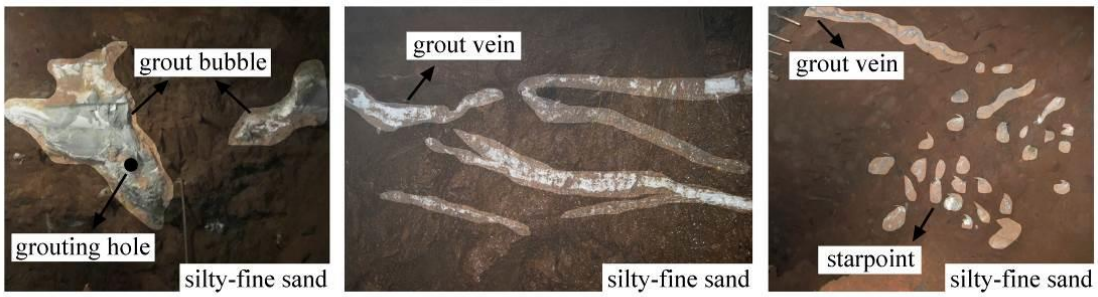

(a) Grout bubble (b) Grout vein (c) Grout vein and starpoint

Fig. 10 The concretions of grout after the excavation

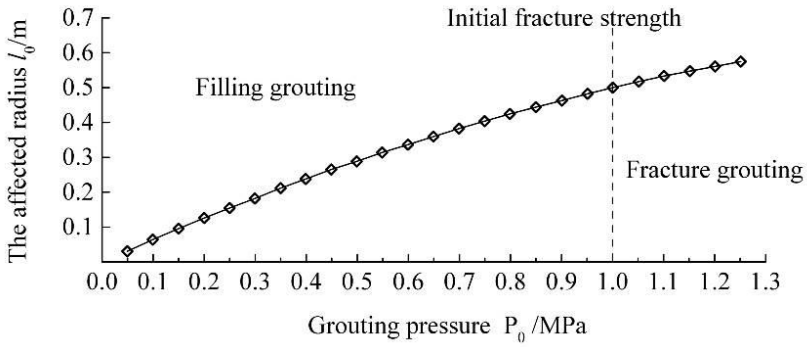

Fig. 11 Relationship between grouting pressure and affected radius

is a process of splitting and the grouting pressure is very important. Fig.11 shows the relationship between grouting pressure P_0 and its affecting radius l_0. When the grouting pressure is less than 1.0 MPa, the permeation and compaction grouting occur, but this permeation is that the slurry enters into the pore or crack of the silty-fine sand disturbed by borehole, which gathers around this hole in a shape of grout bubble, and the affected area is less than 0.5 m. If the grouting pressure is greater than 1.0 MPa, the fracture of soil occurs, and this pressure is the initiation fracture pressure which is larger than the fracture strength of soil. If the grouting pressure is greater than 1.25 MPa, the grout splits the silty-fine sand at a higher pressure like an axe, and forms grouting concretions in the shape of block and vein or star point around the grouting hole. After grouting, similar to clay grouting, the silty-fine sand forms a composite soil composed of compacted sand and grout of various shapes, i.e., the grout is not mixed with the sand particles thoroughly, but exists respectively. Thus, the grouting of the silty-fine sand with abundant water can be regarded as fracture grouting. The numerical simulation of grouting mechanism and practice fully verifies this point.

As mentioned above, the grouting effect is satisfied only after the grouting pressure reaches initiation fracture pressure. In this case, the final grouting pressure is 1.5MPa which is greater than 1.25 MPa. But, if the grouting pressure is too large, it may affect the safety of buildings and underground pipelines around the tunnel. Therefore, the factors such as the grouting amount, the safety of environment around the tunnel, should be taken into considered for the determination of the grouting pressure.

6. Conclusions

According to the study of this paper, the following conclusions are drawn:

1) The grouting of the silty-fine sand with abundant water is a process of splitting. The lack of pressure during grouting is difficult to meet the requirements of excavation. If the pressure during grouting is bigger enough, the soil is split and compacted, and then the soil can be improved significantly.

2) Fracture pressure is a governing parameter for splitting. PFC^{3D} simulation and theoretical calculation showed that fracture pressure of the silty-fine sand with abundant water can be set as 1 MPa, which has been verified by practice.

3) The heavily affected area of grouting is about 0.5 m, and the suitable space between the grouting hole can be set as 0.5 m. The grouting effect of the silt fine sand strata is the best within a diameter of 1 m. The soil is compacted beyond 1m in a certain.

4) Simulation of PFC^{3D} and field observation after excavation show that the concretions of grout are in a shape of block and vein or star point, and the concretions of grout form a composite soil with the silty-fine sand. The composite soil has higher strength and better water stop, which can guarantee the tunnel to be excavated safely.

The grouting technique mentioned above has been used in the excavation of subsequent tunnels. The monitoring of surroundings nearby this tunnel indicates that the settlement of building is only 3.3 mm. Therefore, it can be concluded that this grouting technique can not only make the tunnel to

be excavated successfully, but also keep the surroundings in safety.

Acknowledgments

This paper was supported by Beijing Municipal Natural Science Foundation-Key Project of Beijing Municipal Education commission (KZ201810016021).

References

Amnieh, H.B., Masoudi, M. and Karbala, M. (2017), "Evaluating analytical and statistical models in order to estimate effective grouting pressure", *Comput. Concrete*, **20**(3), 275-282. https://doi.org/10.12989/cac.2017.20.3.275.

Bezuijen, A., Te Grotenhuis, R., Van Tol, A.F., Bosch, J.W. and Haasnoot, J.K. (2011), "Analytical model for fracture grouting in sand", *J. Geotech. Geoenviron. Eng.*, **137**(6), 611-620. https://doi.org/10.1061/(ASCE)GT.1943-5606.0000465.

Björn, S. and Gustafson, G. (2010), "A review of the namntall tunnel project with regard to grouting performance", *Tunn. Undergr. Sp. Tech.*, **25**(4), 346-356. https://doi.org/10.1016/j.tust.2010.01.009.

Cho, G.C., Lee, J.S. and Santamarina, J.C. (2004), "Spatial variability in soils: high resolution assessment with electrical needle probe", *J. Geotech. Geoenviron. Eng.*, **130**(8), 843-850. https://doi.org/10.1061/(ASCE)1090-0241(2004)130:8(843).

Do, N.A., Dias, D., Oreste, P. and Djeran-Maigre, I. (2014), "Three-dimensional numerical simulation for mechanized tunnelling in soft ground: the influence of the joint pattern", *Acta Geotechnica*, **9**(4), 673-694. https://doi.org/10.1007/s11440-013-0279-7.

Fatih, C. (2019), "The observation of permeation grouting method as soil improvement technique with different grout flow models", *Geomech. Eng.*, **17**(4), 367-374. https://doi.org/10.12989/gae.2019.17.4.367.

Jorne, F. and Henriques, F.M.A. (2016), "Evaluation of the grout injectability and types of resistance to grout flow", *Constr. Build. Mater.*, **122**, 171-183. https://doi.org/10.1016/j.conbuildmat.2016.06.032.

Jun, L., Gang, L. and Hongsong, X. (2015), Construction technology of dynamic grouting of subway tunnel in fine-sand with abundant water. Construction Technology.

Ke, W.U., Mingyue, M.A. and Yue, S. (2012), "Evaluation on effects of the change of hole-boring distance during splitting grouting to earth dam", *J. Civil Archit. Environ. Eng.*, **34**(6), 104-108.

Kim, Y.U., Park, J., Chun, Y.W. and Zhang, G.M. (2013), "Evaluation and prediction of physical properties of pressure grouting using laboratory testing and elastic wave velocity", *J. KSCE J. Civil Eng.*, **17**(2), 364-367. https://doi.org/10.1007/s12205-013-1814-7.

Kodam, M., Bharadwaj, R., Curtis, J., Hancock, B. and Wassgren, C. (2009), "Force model considerations for glued-sphere discrete element method simulations", *Chem. Eng. Sci.*, **64**(15), 3466-3475. https://doi.org/10.1016/j.ces.2009.04.025.

Le, H., Sun, S. and Wei, J. (2019), "Influence of types of grouting materials on compressive strength and crack behavior of rocklike specimens with single grout-infilled flaw under axial loads", *J. Mater. Civil Eng.*, **31**(1). https://doi.org/10.1061/(ASCE)MT.1943-5533.0002554.

Lee, H.B., Oh, T.M., Park, E.S., Lee, J.W. and Kim, H.M. (2017), "Factors affecting waterproof efficiency of grouting in single rock fracture", *Geomech. Eng.*, **12**(5), 771-783. https://doi.org/10.12989/gae.2017.12.5.771.

Loveridge, F., Powrie, W. and Nicholson, D. (2014), "Nicholson, Duncan. Comparison of two different models for pile thermal response test interpretation", *Acta Geotechnica*, **9**(3), 367-384. https://doi.org/10.1007/s11440-014-0306-3.

Sadek, M.A., Chen, Y. and Liu, J. (2011), "Simulating shear behavior of a sandy soil under different soil conditions", *J. Terramechanics*, **48**(6), 451-458. https://doi.org/10.1016/j.jterra.2011.09.006.

Silva, R.A., Oliveira, D.V., Schueremans, L., Miranda, T. and Machado, J. (2016), "Effectiveness of the repair of unstabilised rammed earth with injection of mud grouts", *Constr. Build. Mater.*, **127**, 861-871. https://doi.org/10.1016/j.conbuildmat.2016.10.064.

Stille, H., Gustafson, G. and Hassler, L. (2012), "Application of new theories and technology for grouting of dams and foundations on rock", *Geotech. Geol. Eng.*, **30**(3), 603-624. https://doi.org/10.1007/s10706-012-9512-7.

Sun, F., Zhang, D. and Yao, H. (2010), "Study of effects of split grouting for reinforcing bottom of embankment", *Rock Soil Mech.*, **31**(4), 1187-1192.

Suwansawat, S. and Einstein, H.H. (2007), "Describing settlement troughs over twin tunnels using a superposition technique", *J. Geotech. Geoenviron. Eng.*, **133**(4), 445-468. https://doi.org/10.1061/(ASCE)1090-0241(2007)133:4(445).

Zhang, D.M., Huang, Z.K., Wang, R.L., Yan, J.Y. and Zhang, J. (2018), "Grouting-based treatment of tunnel settlement: Practice in Shanghai", *Tunn. Undergr. Sp. Tech.*, **80**, 181-196. https://doi.org/10.1016/j.tust.2018.06.017.

GC